Original Article

Echocardiographic Evaluation of Coronary Abnormalities and Cardiac Function in a Murine Model of Kawasaki Disease Using High-frequency Ultrasound

Xin-Xin Zhang[1,2], Zhong-Dong Du[1,2], Shang-Guan Wen[3], Xiu-Ping Sun[4]

[1]Department of Cardiology, Beijing Children's Hospital, Capital Medical University, Beijing 100045, China
[2]Key Laboratory of Major Disease in Children, Ministry of Health, Beijing 100045, China
[3]Pediatric Cardiac Intensive Center, Beijing Anzhen Hospital, Capital Medical University, Beijing 100029, China
[4]Chinese Academy of Medical Sciences and Comparative Medical Center, Beijing 100021, China

Abstract

Background: Murine model of coronary arterial inflammation has been widely accepted as an animal model of and used in Kawasaki disease (KD). This study sought to evaluate the developmental changes of coronary arteries and cardiac function in a murine model of KD with a high-frequency ultrasound system and to provide evidence for the preparation of the model of KD.

Methods: *Lactobacillus casei* cell wall extract was prepared and injected into C57BL/6 mice intraperitoneally (i.p.) to induce KD. A total of 120 mice were grouped into three groups. The intravenous immunoglobulin (IVIG) treatment group was i.p. injected with IVIG (2 g/kg), while the KD model and normal control groups were i.p. injected with 0.5 ml of phosphate buffered solution on day 5. All high-resolution echocardiography detection of mouse heart was performed by the same senior technician. Animal echocardiography was performed by measuring the coronary artery dimensions and cardiac function on days 0, 7, 14, 28, and 56 (high-resolution small animal ultrasound [Vevo770 pattern; VisualSonic, Canada] with broadband probe [RMVTM707B; frequency, 30 mHz; depth of focus, 1.2 cm]) which were measured and analyzed with Vevo770 software.

Results: Pathological studies revealed focal inflammatory infiltrate asymmetrically distributed around the coronary artery trunk in the KD model group. Echocardiographic study including coronary dimension and cardiac function measurements was successfully performed in all subjects. The KD model and IVIG treatment groups showed left coronary artery dilation on days 7, 14, 28, and 56. The diameter of left coronary artery in the KD model group (0.53 ± 0.09 mm; 0.36 ± 0.07 mm; 0.34 ± 0.05 mm; 0.34 ± 0.04 mm) was significantly larger than those of IVIG treatment group (0.22 ± 0.02 mm; 0.28 ± 0.03 mm; 0.26 ± 0.03 mm; 0.27 ± 0.05 mm; 0.26 ± 0.03 mm; all $P < 0.01$) and the normal control group (0.21 ± 0.02 mm; 0.22 ± 0.03 mm; 0.22 ± 0.02 mm; 0.23 ± 0.02 mm; 0.27 ± 0.04 mm; all $P < 0.01$) on days 7, 14, 28, and 56. No significant differences were observed in the measurements of cardiac function among the groups on days 0, 7, 14, 28, and 56 (all $P > 0.05$).

Conclusions: Echocardiography could identify the consecutive changes of coronary artery in KD mice. Echocardiography is more convenient and direct in evaluating the coronary abnormalities in this animal model.

Key words: Disease Model; Echocardiography; Kawasaki Disease; Murine

Introduction

Kawasaki disease (KD) is a systemic vascular inflammatory disease that usually occurs in childhood. Its incidence has increased in recent years.[1,2] Coronary artery lesions (CALs) are the main complications of KD which have replaced rheumatic fever as the most common pediatric acquired heart disease.[3-5] Coronary artery stenosis or occlusion is a long-term complication of coronary artery aneurysms (CAAs)

Access this article online

Quick Response Code:

Website: www.cmj.org

DOI: 10.4103/0366-6999.207461

Address for correspondence: Dr. Zhong-Dong Du, Department of Cardiology, Beijing Children's Hospital, Capital Medical University, Beijing 100045, China
Key Laboratory of Major Disease in Children, Ministry of Health, Beijing 100045, China
E-Mail: duzhongdong@126.com

Received: 22-01-2017 **Edited by:** Yi Cui
How to cite this article: Zhang XX, Du ZD, Wen SG, Sun XP. Echocardiographic Evaluation of Coronary Abnormalities and Cardiac Function in a Murine Model of Kawasaki Disease Using High-frequency Ultrasound. Chin Med J 2017;130:1467-74.

that causes death or disability. Therefore, KD is a serious disease that affects children's physical and mental health.[6,7]

The etiology and pathogenesis of KD are not clearly elucidated. The establishment and analysis of KD animal model in mice are helpful in investigating its pathogenesis. This model was applied based on the experimental study of KD. The pathological change in the coronary artery and the reaction to intravenous immunoglobulin (IVIG) in the KD murine model induced by intraperitoneal (i.p.) injection of *Lactobacillus casei* cell wall extract (LCWE) are consistent with those observed in children with KD in clinical settings. This animal model of KD with CALs is relatively mature. In 1983, Lehman *et al*.[8] used ultrasonic crushing method to obtain LCWE, which was i.p. injected into C57BL/6 mice. These mice were the first successful coronary artery inflammation model in the United States. Our group has successfully replicated this model with minor modification of the method.[9]

Evaluation of the preparation of the KD murine model mainly depends on the pathology results. This invasive method cannot be performed repetitively. With the development of ultrasonic detection technology in recent years, high-frequency animal cardiac ultrasonography as a noninvasive method has been used to examine various heart diseases in the murine model.[10] However, there are limited data in literature on the echocardiographic studies about the KD murine model of coronary artery pathological changes.

In this study, the KD murine model was induced by LCWE. A high-frequency small animal cardiac ultrasound instrument was used to observe the dynamic changes of the CALs of the KD murine model dynamically. It was also employed to evaluate the diagnostic value in the KD murine model.

Methods

Experimental animals

C57BL/6 mice (male, 3–4 weeks old, 12.6 ± 0.8 g weight) were purchased from Chinese Academy of Medical Sciences and Comparative Medical Center (Certificate of Quality No: SYXK [Beijing] 2014-0023). The mice were raised under specific pathogen-free conditions at the Department of Laboratory Animals of Chinese Academy of Medical Sciences and Comparative Medical Center. All animal studies and protocols were approved by the Institutional Animal Care and Use Committee of Chinese Academy of Medical Sciences and Comparative Medical Center.

Kawasaki disease model preparation and treatment

The murine model of KD was prepared as previously described by Duong *et al*.[11] Briefly, *L. casei* (ATCC 11578) cultured in lactobacilli MRS broth (oxid, Britain) was harvested using centrifugation (9600 ×*g*, 30 min) during the log phase of growth and lysed with 4% sodium dodecyl sulfate (SDS, Sigma Systems, USA). Sequential incubations with 250 μg/ml RNase, DNase I and trypsin (Sigma Systems, USA) were performed to remove any adherent material from the cell walls. After centrifugation, the pellet was sonicated (1 g packed wet weight in 3 ml phosphate buffered saline [PBS]) and further centrifuged with the resultant supernatant containing the LCWE.

A total of 120 mice were grouped into three groups with 40 mice in each group randomly. Eighty mice were i.p. injected with 0.5 mg of LCWE in 0.5 ml of PBS to induce KD model. The control group was i.p. injected with 0.5 ml PBS alone on day 0. The IVIG treatment group was i.p. injected with IVIG (2 g/kg; HualanBio, China) on day 5, and the KD model and normal control groups were i.p. injected with 0.5 ml of PBS. According to the pathological changes in the KD murine model,[10] all the mice were ultrasonically observed for the developmental changes of coronary arteries and cardiac function on days 0, 7, 14, 28, and 56.

High-resolution echocardiography detection of mouse heart

Three bromine ethanol (0.2 ml/10 g·weights) were used for the i.p. injection of anesthesia. After the anesthetization, the left chest area was besmeared with hair removal cream for 1 min and wiped clean with a swab. Subsequently, the mice were placed supine, and ultrasonic coupling agent was applied on their chests. The left sternum was selected for long and short axis evaluation by ultrasonography (high-resolution small animal ultrasound [Vevo770 pattern; VisualSonic, Canada] with broadband probe [RMVTM707B; frequency, 30 mHz; depth of focus, 1.2 cm]).

The end-diastolic trunk diameters of the left and right coronary arteries were ultrasonically measured in all mice on days 0 (before making KD model), 7, 14, 28, and 56. When CAAs occurred, their sizes and scopes were measured. The diagnostic criteria of the American Heart Association were used for the standard diagnosis of CAAs,[3] that is, the inner diameter of a section expanded more than 1.5-times than the adjacent inner diameter. Three consecutive cardiac cycles were recorded to extract the parameters of the ultrasonic storage in mice, which were measured and analyzed with Vevo770 software.

Histological examination

Ten mice of each group were killed by decapitation after echocardiography detection on days 7, 14, 28, 56. Cardiac tissues for evaluation of inflammatory reaction were fixed in 10% paraformaldehyde for 24 h. Serial paraffin sections (5 μm) were prepared, stained with hematoxylin and eosin and elastin-van Gieson, and then examined by light microscopy (×200).

Statistical analysis

Data were presented as mean ± standard deviation (SD) and statistically analyzed using SPSS version 22.0 software (SPSS, Inc., Chicago, IL, USA) and Prism4 software (GraphPad, San Diego, CA, USA). Differences were compared using one-way analysis of variance. A value of $P < 0.05$ was considered statistically significant.

Results

Appearance commonly observed in mice

Approximately, 12 h following injection of LCWE, mice exhibited decreases in food intake and locomotor activity. Moreover, some mice appeared shivering. After 1–2 days, shivering gradually disappear. During the following days, food consumption in the KD model group recovered gradually, while the level of locomotor activity remained decreased throughout the duration of the experimental period.

Coronary artery lesions in experimental Kawasaki disease

To evaluate the inflammatory reaction of cardiac tissues, 10 mouse hearts were harvested on days 7, 14, 28, and 56 in each group after echocardiographic detection by decapitation. A focal inflammatory infiltrate was evident in the coronary artery trunk. The inflammatory cell infiltrates consisted of mononuclear lymphocytes, which concentrated asymmetrically around the tunica adventitia of the coronary artery in the KD model and IVIG treatment group on days 7 and 14 [Figure 1a and 1b]. Disruption of elastin was consistently observed on days 28 and 56 in the KD model group [Figure 1c]. In the normal control group, inflammatory infiltrate in the coronary trunk was not observed, and the elastin of the coronary artery was clear and continuous on days 28 and 56 [Figure 1d]. Thus, the model was successfully created, and the IVIG treatment was effective, which is consistent in the clinical practice.

Echocardiographic detection of coronary arteries

The left and right coronary arteries of all mice were detected. Forty mice of the KD model group (100%) showed coronary artery dilatation, coarse endometrium, and partially irregular lumen. Some of the left coronary arteries in the KD model group (7 in 40, 17.5%) exhibited CAA-like ectasia changes. Combined with the pathological examination results, the success rate of the created model was up to 100%.

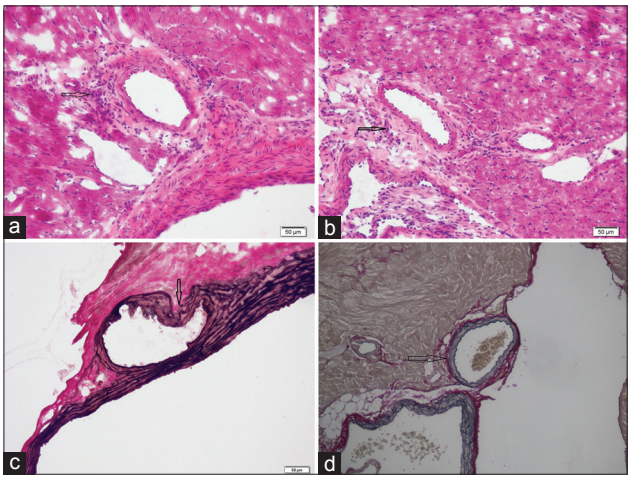

Figure 1: Pathological images of mouse heart. Arrow indicates focal inflammatory infiltrate asymmetrically distributed around the coronary artery trunk in the Kawasaki disease model and intravenous immunoglobulin treatment group on days 7 and 14 (stained with hematoxylin and eosin; a and b). Arrow indicates the disruption of elastin that was consistently observed on day 56 in the Kawasaki disease model group (stained with elastic van Gieson; c). The elastin of the coronary artery was clear and continuous in the normal control group (d). Scale bar represents 50 μm.

Echocardiographic detection of coronary arteries on day 0

Before making KD model, echocardiography showed that the coronary artery vessel walls of the three groups presented fine linear echo, which had intensity lower than the aortic root on day 0. The inner vascular layer of the coronary artery was smooth, and the outer pipe walls were clear from the surrounding adjacent tissue boundaries without CALs. No significant differences were observed in the measurements of left and right coronary artery diameter among the three groups (all $P > 0.05$; Tables 1 and 2).

Echocardiographic detection of coronary arteries on day 7

Echocardiography showed that the coronary artery vessel walls of the normal control group presented fine linear echo, which had intensity lower than the aortic root on day 7. The inner vascular layer of the coronary artery was smooth, and the outer pipe walls were clear from the surrounding adjacent tissue boundaries without coronary dilation [Figure 2a].

The echocardiography of the KD model group exhibited that the echogenicity of the surrounding coronary artery walls and pipe walls was enhanced and significantly higher

Table 1: Comparison of the left coronary artery diameter (mm)

Variables	KD model group	IVIG treatment group	Normal control group
Day 0	0.21 ± 0.03	0.22 ± 0.02*	0.21 ± 0.02*,‡
Day 7	0.53 ± 0.09	0.28 ± 0.03†	0.22 ± 0.03†,§
Day 14	0.36 ± 0.07	0.26 ± 0.03†	0.22 ± 0.02†,§
Day 28	0.34 ± 0.05	0.27 ± 0.05†	0.23 ± 0.02†,§
Day 56	0.34 ± 0.04	0.26 ± 0.03†	0.27 ± 0.04†,‡

Values are expressed as mean ± SD. $n = 10$ in each group. Compared with the KD model group: *P>0.05, †P<0.05; Compared with the IVIG treatment group: ‡P>0.05, §P<0.05. SD: Standard deviation; KD: Kawasaki disease; IVIG: Intravenous immunoglobulin.

Table 2: Comparison of the right coronary artery diameter (mm)

Variables	KD model group	IVIG treatment group	Normal control group
Day 0	0.18 ± 0.04	0.17 ± 0.02*	0.17 ± 0.03*,‡
Day 7	0.28 ± 0.02	0.25 ± 0.03†	0.18 ± 0.03†,§
Day 14	0.27 ± 0.04	0.21 ± 0.03†	0.18 ± 0.03†,§
Day 28	0.25 ± 0.05	0.22 ± 0.05*	0.19 ± 0.02†,§
Day 56	0.29 ± 0.05	0.23 ± 0.03†	0.21 ± 0.03†,‡

Values are expressed as mean ± SD. $n = 10$ in each group. Compared with the KD model group: *P>0.05, †P<0.05; Compared with the IVIG treatment group: ‡P>0.05, §P<0.05. SD: Standard deviation; KD: Kawasaki disease; IVIG: Intravenous immunoglobulin.

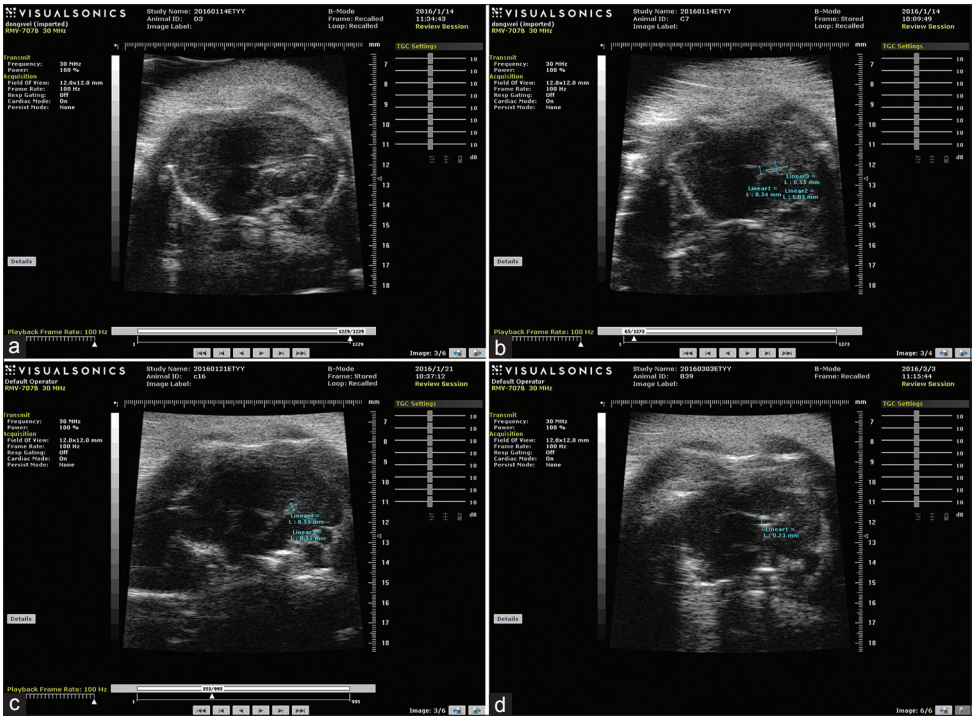

Figure 2: High-resolution echocardiography detection of coronary arteries of mouse heart. Day 7 after *Lactobacillus casei* cell wall extract injection. (a) The echocardiography of the normal control group showed a smooth coronary artery wall. (b) The echocardiography of the Kawasaki disease model group exhibited a noticeable blur in the coronary artery intima and concomitant with left coronary artery aneurysm-like ectasia changes. Day 14 after *Lactobacillus casei* cell wall extract injection. (c) The echocardiography of the Kawasaki disease model group showed irregular with plaque and coronary artery aneurysm-like ectasia changes. Day 28 after *Lactobacillus casei* cell wall extract injection. (d) The echocardiography of the Kawasaki disease model group showed a clear echogenicity of the coronary artery wall and presented a plate-shaped enhancement.

than that of the aortic root. Moreover, the echo of the part of the blood vessel edge and its surrounding was unclear, and plate-shaped echogenicity was enhanced on day 7. Two mice of the KD model group ($n = 10$, 20%) showed left CAA-like ectasia changes [Figure 2b]. The mean value of the maximum cross-sectional area of the CAAs was 0.34 mm^2.

The echocardiography of the IVIG treatment group was similar to that of the KD model group; one mouse ($n = 10$, 10%) showed CAA-like ectasia changes. The mean value of the maximum cross-sectional area of the CAA was 0.27 mm^2. The mean of the left and right coronary artery diameters of the KD model on day 0 (0.21 ± 0.03 mm, 0.18 ± 0.04 mm) was significantly smaller than on day 7 (0.53 ± 0.09 mm, 0.28 ± 0.02 mm; all $P < 0.01$; Tables 1 and 2). The left coronary artery diameter of the KD model group (0.53 ± 0.09 mm) was significantly larger than that of the normal control group (0.22 ± 0.03 mm, $P = 0.000$) and the IVIG treatment group (0.28 ± 0.03 mm, $P = 0.000$; Table 1 and Figure 3a). The right coronary artery diameter of the KD model group (0.28 ± 0.02 mm) was larger than that of the normal control group (0.18 ± 0.03 mm, $P < 0.05$) and the IVIG treatment group (0.25 ± 0.03 mm, $P < 0.05$; $n = 10$ in each group; Table 2 and Figure 3b).

Echocardiographic detection of coronary arteries on day 14

The echocardiography expression of the normal control group exhibited no evident changes between days 14 and 7. The echo of the KD model group showed that the surrounding coronary artery walls and pipe walls strengthened on day 14 than on day 7. The echo of the blood vessel part and its outer surrounding was unclear and presented a plate-shaped enhancement, which was coarse and exhibited an irregular lumen. The proximal left main coronary arteries of 3 mice showed aneurysm-like dilation changes [Figure 2c]. The mean value of the maximum cross-sectional area of the CAAs was 0.28 mm^2. The echocardiography of the IVIG treatment group was similar to the KD model group but without coronary dilation.

The left coronary artery diameter of the KD model group (0.36 ± 0.07 mm) was significantly larger than that of the normal control group (0.22 ± 0.02 mm, $P = 0.000$). It was also larger than that of the IVIG treatment group (0.26 ± 0.03 mm, $P = 0.000$; Table 1 and Figure 3c). The right coronary artery diameter of the KD model group (0.27 ± 0.04 mm, $P < 0.05$) was larger than that of the normal control group (0.18 ± 0.03 mm) and the IVIG treatment group (0.21 ± 0.03 mm, $P < 0.05$; $n = 10$ in each group; Table 2 and Figure 3d).

Echocardiographic detection of coronary arteries on day 28

The echocardiography of the coronary arteries of the normal control group showed similar results on day 28 as before. The echo showed that the surrounding coronary artery walls and pipe walls of the KD model group were more reduced

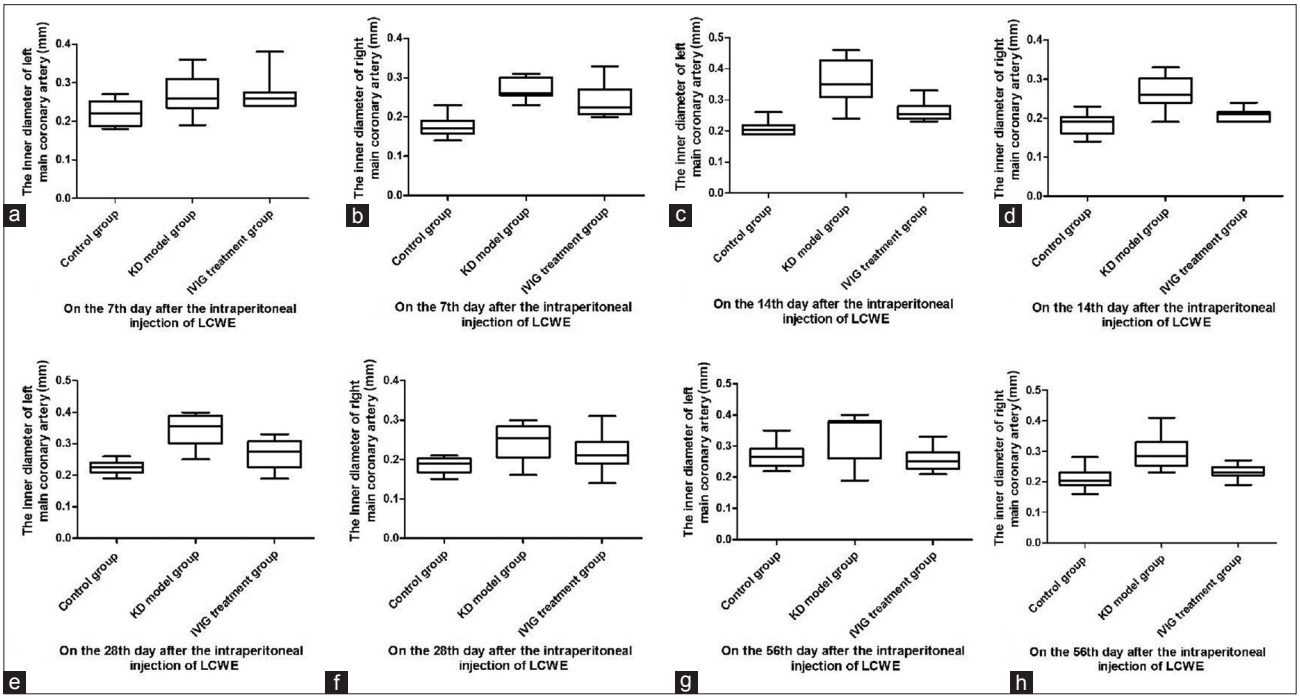

Figure 3: Coronary arteries inner diameters comparison. The box plot shows inner diameters of the left and right main coronary arteries of the control, Kawasaki disease model and intravenous immunoglobulin treatment groups on day 7 (a and b; all $P < 0.05$); on day 14 (c and d; all $P < 0.05$); on day 28 (e and f); and on day 56 (g and h).

on day 28 than on day 14. The echo of the blood vessel part and its outer surrounding was clear and presented a plate-shaped enhancement. The proximal left main coronary arteries of one mouse showed aneurysm-like dilation changes [Figure 2d]. The mean value of the maximum cross-sectional area of the CAA was 0.25 mm^2. Compared with the KD group, echocardiography showed that the echogenicity of the surrounding and outer blood vessel edge of the IVIG treatment group did not evidently increase. In addition, the vascular intima was slightly coarse and the lumen was relatively regular.

Meanwhile, the left coronary artery diameter of the KD model group (0.34 ± 0.05 mm) was significantly larger than that of the normal control group (0.23 ± 0.02 mm, $P = 0.000$). It was also larger than that of the IVIG treatment group (0.27 ± 0.05 mm, $P = 0.000$; Table 1 and Figure 3e). The right coronary artery diameter of the KD model group (0.25 ± 0.05 mm) was larger than that of the normal control group (0.19 ± 0.02 mm, $P = 0.001$) and the IVIG treatment group (0.22 ± 0.05 mm, but $P > 0.05$; Table 2 and Figure 3f; $n = 10$ in each group).

Echocardiographic detection of coronary arteries on day 56

The coronary artery ultrasonography of the normal control group was similar on day 56 as before. The echocardiography of the KD model group on day 56 showed that the echogenicity of the surrounding coronary artery walls and pipe walls was strengthened. However, diffuse thickening and lumen stenosis of some coronary artery walls were observed. The proximal left main coronary arteries of one murine showed aneurysm-like dilation changes (0.26 mm × 0.47 mm). The echocardiography of the IVIG treatment group was similar to that of the normal group without coronary dilation.

The left coronary artery diameter of the KD model group (0.34 ± 0.04 mm) was larger than that of the normal control group (0.27 ± 0.04 mm, $P = 0.000$) and IVIG treatment group (0.26 ± 0.03 mm, $P = 0.000$). However, no statistically significant difference was found between the IVIG treatment and normal control groups ($P > 0.05$; Table 1 and Figure 3g). The right coronary artery diameter of the KD model group (0.29 ± 0.05 mm) was larger than that of the normal control group (0.21 ± 0.03 mm) and the IVIG treatment group (0.23 ± 0.03 mm), with statistically significant difference ($P = 0.000$, $P = 0.001$). No statistically significant difference was observed between the IVIG treatment and normal control groups ($P > 0.05$; $n = 10$ in each group; Table 2 and Figure 3h).

Echocardiographic detection of cardiac function on days 0, 7, 14, 28, and 56

The cardiac function of all mice including left ventricular end-diastolic diameter (LVID d), left ventricular end-systolic diameter (LVID s), left ventricular end-diastolic volume (LV Vol d), left ventricular end-systolic volume (LV Vol s), left ventricular end-diastolic posterior wall thickness (LVPW d), left ventricular end-systolic posterior wall thickness (LVPW s), left ventricular end-diastolic anterior wall thickness (LVAW d), left ventricular end-systolic anterior wall thickness (LVAW s), ejection fraction (EF), fractional shortening (FS), and stroke volume (SV) was

assessed on days 0, 7, 14, 28, and 56. No significant differences were observed in the measurements of cardiac function including LVID d, LVID s, LV Vol d, LV Vol s, LVPW d, LVPW s, LVAW d, LVAWs, EF, FS, and SV among the groups on days 0, 7, 14, 28, and 56 (all $P > 0.05$; Tables 3–5).

Discussion

The cause and pathogenesis of KD are not completely elucidated. Numerous studies have investigated infection-induced immune mechanisms that cause inflammation of the middle and small systemic arteries.[12,13] Most prognoses of children with KD are satisfactory, and pathologic specimens are difficult to obtain. Thus, establishing a KD animal model is an important method to further research on KD etiology and accompanying pathogenesis of CALs.

In the present study, a murine model of KD-induced by a single i.p. injection of LCWE was shown to exhibit similar CALs to KD patients with CAAs.[11] CALs in KD is a dynamic evolution process. A previous study performed pathological observation of the changes in CALs as an evaluation method.[11] However, this method is difficult to repeat and cannot observe the changes of CALs in mice continuously and dynamically, thus limiting the further study of KD. With the development of high-frequency ultrasound probe techniques and high-frame-frequency technology image acquisition in recent years, murine cardiac ultrasound image quality has significantly improved. Cardiac ultrasound as a noninvasive method has been used for examination in various heart diseases in the murine model.[10]

In this study, the high-frequency animal ultrasound instrument was used for dynamic observation and comprehensive evaluation of the CALs of the KD model in different stages. Clear images were detected in all mice and provided an effective method to evaluate the CALs of the KD model. This research observed the change in CALs by measuring and calculating the average coronary artery diameters, as well as comparing the differences among the groups.

The results showed that no significant differences were observed in the measurements of left and right coronary artery diameter among the three groups on day 0, before making KD model. The mean of the left and right coronary artery diameters of the KD model on day 0 was significantly smaller than on day 7. It was showed that the mean of the left coronary artery diameters of the KD model and IVIG treatment groups was significantly larger than that of the normal control group on days 7, 14, 28, 56. The ultrasonic cardiogram of the KD model group showed that the CALs slowly gradually improved but a few of them with the sequelaes of artery wall lining diffuse thickening and lumen stenosis and even aneurysm. The left CALs of the IVIG treatment group were slightly similar to those of the KD model group on the acute stage but improved rapidly on the following days with the coronary artery wall lining and lumen relatively regular, unobstructed. The left coronary artery diameters of the IVIG treatment and normal control groups exhibited no difference at the end of the experiment. The results were similar to KD in children with CALs and prompted that the IVIG treatment reaction of the KD murine model was analogous to the clinical manifestation of children with KD.

The diagnostic criteria of CAA established by the American Heart Association were used in this study.[3] In the KD model group, 2, 3, 1, 1 mice were concomitant with left CAA-like ectasia changes on days 7, 14, 28, 56, respectively. The mean value of the maximum cross-sectional area of the CAA was reduced gradually on days 14, 28, 56 than before. The echocardiography of the IVIG treatment group was analogous to the KD model group, with one mouse concomitant with CAA-like ectasia changes on day 7. CAA-like ectasia changes were not observed on days 14, 28, and 56 in IVIG treatment group. Notably, the broadening diameter of the left main coronary artery was more obvious in the KD model group, and all the CAA-like ectasia changes were found in the left coronary arteries. The trunk diameter of the right coronary artery of the KD model group was wider than that of the normal control group but without aneurysm-like ectasia change.

Moreover, the cardiac function including LVID d, LVID s, LV Vol d, LV Vol s, LVPW d, LVPW s, LVAW d, LVAW s, EF, FS, and SV was assessed on days 0, 7, 14, 28, and 56. However, there were no significant differences among the groups on days 0, 7, 14, 28, and 56.

This study suggests that LCWE-induced C57BL/6 murine KD model is more likely to involve the left coronary arteries, but the specific reasons need to be further investigated. The coronary artery diameters of the IVIG treatment group gradually returned to normal. Compared with the KD model group at different time points, statistically significant difference was observed between them. IVIG is effective in the treatment of KD murine model and can be dynamically monitored by echocardiography.

This study has several limitations. KD is not only involved in the main coronary arteries, but also in the branches. Given the limitation of ultrasonic probe frequency, this study cannot detect the lesions of the distal coronary artery in mice. However, the trunk and proximal branch are also involved when lesions are present in the distal end because KD is complicated with CALs that mostly occur in the proximal end.[3] The diagnosis of KD complicated with CALs remains accurate.

In this study, preliminary observation on the dynamic changes of the coronary artery of the three groups was conducted using high-frequency small animal cardiac ultrasound. The coronary artery ultrasound showed clear images of nearly all the mice. This result indicates that the evaluation of the changes in CALs in the KD murine model by high-frequency small animal ultrasound is feasible. Meanwhile, it shows that the recovery and changes of IVIG

Table 3: Cardiac function assessment of the IVIG treatment group

Variables	Day 0	Day 7	Day 14	Day 28	Day 56
LVID d (mm)	3.46 ± 0.16	3.48 ± 0.1	3.61 ± 0.18	3.61 ± 0.26	3.87 ± 0.17
LVID s (mm)	2.20 ± 0.20	2.00 ± 0.21	2.12 ± 0.31	2.26 ± 0.28	2.32 ± 0.50
LV Vol d (μl)	51.87 ± 5.76	50.62 ± 3.19	55.13 ± 6.73	65.41 ± 9.48	67.78 ± 6.80
LV Vol s (μl)	13.58 ± 3.61	13.05 ± 3.34	15.27 ± 5.43	17.92 ± 5.75	21.61 ± 5.26
LVPW d (mm)	0.60 ± 0.06	0.62 ± 0.07	0.63 ± 0.07	0.63 ± 0.07	0.68 ± 0.10
LVPW s (mm)	1.02 ± 0.14	1.01 ± 0.09	1.08 ± 0.13	1.02 ± 0.87	1.11 ± 0.15
LVAW d (mm)	0.73 ± 0.12	0.72 ± 0.09	0.80 ± 0.10	0.86 ± 0.16	0.86 ± 0.10
LVAW s (mm)	1.14 ± 0.15	1.21 ± 0.12	1.24 ± 0.13	1.25 ± 0.22	1.32 ± 0.17
SV (μl)	38.52 ± 4.26	38.47 ± 3.16	39.86 ± 5.84	43.50 ± 7.09	44.15 ± 4.49
EF (%)	72.68 ± 4.87	74.81 ± 5.86	72.58 ± 8.69	69.57 ± 6.41	70.91 ± 5.83
FS (%)	41.27 ± 4.25	43.08 ± 5.26	41.50 ± 7.16	41.9 ± 6.48	41.33 ± 4.29
LV mass (AW) (g)	60.82 ± 5.60	59.91 ± 7.07	62.91 ± 7.43	75.94 ± 11.10	84.83 ± 10.48

Values are expressed as mean ± SD. LVID d: Left ventricular end-diastolic diameter; LVIDs: Left ventricular end-systolic diameter; LV Vol d: Left ventricular end-diastolic volume; LV Vol s: Left ventricular end-systolic volume; LVPW d: Left ventricular end-diastolic posterior wall thickness; LVPW s: Left ventricular end-systolic posterior wall thickness; LVAW d: Left ventricular end-diastolic anterior wall thickness; LVAW s: Left ventricular end-systolic anterior wall thickness; SV: Stroke volume; EF: Ejection fraction; FS: Fractional shortening; SD: Standard deviation; LV: Left ventricular; AW: Anterior wall thickness; IVIG: Intravenous immunoglobulin.

Table 4: Cardiac function assessment of the KD treatment group

Variables	Day 0	Day 7	Day 14	Day 28	Day 56
LVID d (mm)	3.46 ± 0.17	3.48 ± 0.18	3.59 ± 0.20	3.77 ± 0.31	3.84 ± 0.25
LVID s (mm)	2.05 ± 0.23	2.06 ± 0.30	2.11 ± 0.28	2.32 ± 0.35	2.28 ± 0.39
LV Vol d (μl)	50.68 ± 5.46	50.21 ± 5.94	54.48 ± 7.17	62.20 ± 11.09	65.09 ± 8.77
LV Vol s (μl)	13.43 ± 3.68	14.24 ± 5.51	14.93 ± 4.71	19.36 ± 6.22	20.73 ± 6.58
LVPW d (mm)	0.61 ± 0.04	0.62 ± 0.08	0.59 ± 0.04	0.66 ± 0.10	0.67 ± 0.07
LVPW s (mm)	1.01 ± 0.12	1.02 ± 0.12	0.97 ± 0.11	1.01 ± 0.14	1.07 ± 0.13
LVAW d (mm)	0.72 ± 0.06	0.75 ± 0.08	0.76 ± 0.07	0.77 ± 0.12	0.83 ± 0.10
LVAW s (mm)	1.14 ± 0.10	1.20 ± 0.13	1.26 ± 0.10	1.22 ± 0.16	1.31 ± 0.17
SV (μl)	36.50 ± 4.25	35.97 ± 5.94	39.56 ± 3.83	42.24 ± 6.54	43.52 ± 5.93
EF (%)	71.59 ± 4.81	70.12 ± 9.43	71.11 ± 6.00	66.87 ± 5.28	67.55 ± 5.58
FS (%)	41.70 ± 4.12	40.82 ± 7.27	41.64 ± 5.38	40.00 ± 4.98	41.67 ± 4.33
LV mass (AW) (g)	60.90 ± 5.78	60.18 ± 6.55	63.80 ± 9.36	73.14 ± 10.53	81.90 ± 12.57

Values are expressed as mean ± SD. LVID d: Left ventricular end-diastolic diameter; LVIDs: Left ventricular end-systolic diameter; LV Vol d: Left ventricular end-diastolic volume; LV Vol s: Left ventricular end-systolic volume; LVPW d: Left ventricular end-diastolic posterior wall thickness; LVPW s: Left ventricular end-systolic posterior wall thickness; LVAW d: Left ventricular end-diastolic anterior wall thickness; LVAW s: Left ventricular end-systolic anterior wall thickness; SV: Stroke volume; EF: Ejection fraction; FS: Fractional shortening; SD: Standard deviation; LV: Left ventricular; AW: Anterior wall thickness; KD: Kawasaki disease.

Table 5: Cardiac function assessment of the normal control group

Variables	Day 0	Day 7	Day 14	Day 28	Day 56
LVID d (mm)	3.50 ± 0.20	3.58 ± 0.16	3.59 ± 0.27	3.83 ± 0.26	3.91 ± 0.20
LVID s (mm)	2.12 ± 0.18	2.14 ± 0.20	2.16 ± 0.18	2.52 ± 0.24	2.58 ± 0.26
LV Vol d (μl)	52.83 ± 4.92	53.87 ± 5.78	54.66 ± 9.71	67.38 ± 10.67	69.87 ± 9.19
LV Vol s (μl)	14.62 ± 3.58	15.35 ± 3.61	15.72 ± 3.08	22.09 ± 5.15	24.57 ± 6.09
LVPW d (mm)	0.59 ± 0.12	0.60 ± 0.06	0.62 ± 0.05	0.63 ± 0.06	0.73 ± 0.09
LVPW s (mm)	1.00 ± 0.18	1.02 ± 0.10	1.02 ± 0.15	1.04 ± 0.15	1.18 ± 0.17
LVAW d (mm)	0.73 ± 0.13	0.74 ± 0.05	0.73 ± 0.09	0.80 ± 0.09	0.87 ± 0.08
LVAW s (mm)	1.10 ± 0.16	1.13 ± 0.11	1.22 ± 0.15	1.23 ± 0.16	1.32 ± 0.15
SV (μl)	37.78 ± 3.45	38.52 ± 4.14	38.95 ± 7.92	44.30 ± 7.46	45.14 ± 4.56
EF (%)	71.00 ± 4.62	71.68 ± 4.99	71.11 ± 4.42	70.94 ± 5.97	72.98 ± 8.08
FS (%)	39.33 ± 5.15	40.27 ± 4.05	39.81 ± 3.80	40.91 ± 3.96	43.67 ± 7.20
LV mass (AW) (g)	60.79 ± 4.38	61.82 ± 5.67	63.17 ± 14.25	79.08 ± 0.16	84.82 ± 12.73

Values are expressed as mean ± SD. LVID d: Left ventricular end-diastolic diameter; LVIDs: Left ventricular end-systolic diameter; LV Vol d: Left ventricular end-diastolic volume; LV Vol s: Left ventricular end-systolic volume; LVPW d: Left ventricular end-diastolic posterior wall thickness; LVPW s: Left ventricular end-systolic posterior wall thickness; LVAW d: Left ventricular end-diastolic anterior wall thickness; LVAW s: Left ventricular end-systolic anterior wall thickness; SV: Stroke volume; EF: Ejection fraction; FS: Fractional shortening; LV: Left ventricular; AW: Anterior wall thickness; SD: Standard deviation.

treatment of the KD murine model are feasible. The findings provided basis for the preparation and evaluation of KD model and the effectiveness of treatment.

This study also confirmed that the LCWE-induced KD murine model of CALs is similar to the natural course of KD in children with CALs which could simulate the formation process of KD CALs. IVIG treatment of the KD murine model can effectively promote the repair of CAL sand reduce the incidence of CAAs. The treatment is consistent with the clinical manifestations of KD in children.

In conclusion, echocardiography could identify the consecutive changes of coronary artery in KD mice. Echocardiography is more convenient and direct in evaluating the coronary abnormalities in this animal model.

Financial support and sponsorship

Nil.

Conflicts of interest

There are no conflicts of interest.

References

1. Du ZD, Zhao D, Du J, Zhang YL, Lin Y, Liu C, *et al.* Epidemiologic study on Kawasaki disease in Beijing from 2000 through 2004. Pediatr Infect Dis J 2007;26:449-51. doi: 10.1097/01.inf.0000261196.79223.18.
2. Chen JJ, Ma XJ, Liu F, Yan WL, Huang MR, Huang M, *et al.* Epidemiologic features of Kawasaki disease in shanghai from 2008 through 2012. Pediatr Infect Dis J 2016;35:7-12. doi: 10.1097/INF.0000000000000914.
3. Newburger JW, Takahashi M, Gerber MA, Gewitz MH, Tani LY, Burns JC, *et al.* Diagnosis, treatment, and long-term management of Kawasaki disease: A statement for health professionals from the Committee on Rheumatic Fever, Endocarditis and Kawasaki Disease, Council on Cardiovascular Disease in the Young, American Heart Association. Circulation 2004;110:2747-71. doi: 10.1161/01.CIR.0000145143.19711.78.
4. Burns JC. The riddle of Kawasaki disease. N Engl J Med 2007;356:659-61. doi: 10.1056/NEJMp068268.
5. Falcini F. Vascular and connective tissue diseases in the paediatric world. Lupus 2004;13:77-84. doi: 10.1191/0961203304lu517rr.
6. JCS Joint Working Group. Guidelines for diagnosis and management of cardiovascular sequelae in Kawasaki disease (JCS 2013). Digest version. Circ J 2014;78:2521-62. doi: 10.1253/circj.CJ-66-0096.
7. Zhao CN, Du ZD, Gao LL. Corticosteroid therapy might be associated with the development of coronary aneurysm in children with Kawasaki disease. Chin Med J 2016;129:922-8. doi: 10.4103/0366-6999.179801.
8. Lehman TJ, Walker SM, Mahnovski V, McCurdy D. Coronary arteritis in mice following the systemic injection of group B *Lactobacillus casei* cell walls in aqueous suspension. Arthritis Rheum 1985;28:652-9. doi: 10.1002/art.1780280609.
9. Liu JF, Du ZD, Chen Z, Lu DX, Li L, Guan YQ, *et al.* Endothelial progenitor cell down-regulation in a mouse model of Kawasaki disease. Chin Med J 2012;125:496-501. doi: 10.3760/cma.j.issn.0366-6999.2012.03.018.
10. Kanno S, Lerner DL, Schuessler RB, Betsuyaku T, Yamada KA, Saffitz JE, *et al.* Echocardiographic evaluation of ventricular remodeling in a mouse model of myocardial infarction. J Am Soc Echocardiogr 2002;15:601-9. doi: 10.1067/mje.2002.117560.
11. Duong TT, Silverman ED, Bissessar MV, Yeung RS. Superantigenic activity is responsible for induction of coronary arteritis in mice: An animal model of Kawasaki disease. Int Immunol 2003;15:79-89. doi: 10.1093/intimm/dxg007.
12. Rodríguez-Pla A, Stone JH. Vasculitis and systemic infections. Curr Opin Rheumatol 2006;18:39-47. doi: 10.1097/01.bor.0000197999.58073.2e.
13. Kim S, Dedeoglu F. Update on pediatric vasculitis. Curr Opin Pediatr 2005;17:695-702. doi: 10.1097/01.mop.0000187190.97166.83.